



## An investigation on the use of date palm fibers and coir pith as adsorbents for Pb(II) ions from its aqueous solution

Ahmed A. Alghamdi

*Chemical Engineering Technology Department, Yanbu Industrial College, Royal Commission for Jubail and Yanbu, P.O. Box 30436, Yanbu Al-sinaiah, 41912 Yanbu Industrial City, Saudi Arabia, Tel. +966 143213888; email: [alghamdia@rcyci.edu.sa](mailto:alghamdia@rcyci.edu.sa)*

Received 13 January 2015; Accepted 27 April 2015

---

### ABSTRACT

The adsorption process is being widely used for the removal of heavy metals from wastewater streams and many adsorbent materials are being used for this purpose. In recent years, there is a growing need for safe and economical methods for the removal of heavy metals from contaminated waters which demands the utilization of agro-waste-based materials as low-cost adsorbent materials. The present investigation deals with the use of date palm fiber and coir pith for the removal of lead ions (Pb(II)) from wastewater in a laboratory column filtration setup. The concentration of heavy metal from the effluents was analyzed using atomic absorption spectroscopy. Both the adsorbent materials were studied by changing the bed weight under different flow rates. Mathematical modeling of the breakthrough curves was carried out using Thomas model and bed depth service time model equations. The breakthrough curves showed that date palm fibers are having better adsorption efficiency compared to coir pith.

*Keywords:* Adsorption; Date-palm fiber; Coir pith; Mathematical models

---

### 1. Introduction

Contamination problems to drinking water sources are a topic of major concern for developing and underdeveloped countries in recent years. The major sources of contamination come from both industrial and agricultural activities and natural sources. The ground water is mainly polluted with toxic anions, heavy metals, organic compounds, and dyes from the effluents from the industries, and all developing countries are trying to decrease the impact by various means. These toxic chemicals cause health problems when they exceed the tolerance limits in water. The guidelines for drinking water prescribed by the WHO for nitrate, sulfate, molybdenum, selenium, nickel, chromium (VI), and mercury are 50, 250, 0.01,

0.01, 0.02, 0.05, and 0.001 mg/dm<sup>3</sup>, respectively [1]. According to the Bureau of Indian Standards, the discharge limit of vanadium in industrial effluents into surface water is 0.2 mg/dm<sup>3</sup> [2]. In Germany, the applicable limit of phosphates in drinking water is 6.7 mg/dm<sup>3</sup> [3]. Also, the tolerance limit for phenolic compounds in drinking water is 0.001 mg/dm<sup>3</sup> [4]. The above-mentioned values are a few examples of tolerance limits of heavy ions to be present in drinking water.

The presence of toxic ions, heavy metals, and organic compounds in drinking water cause several health problems if consumed for long time. For example, phenolic compounds are said to accelerate tumor formation, cancer and mutation, nickel causes liver damage, chromium (VI) is carcinogenic, sulfates cause

dehydration and catharsis, thiocyanate inhibits the iodine intake causing thyroid problems, and vanadium compounds are harmful to the circulatory system [5–8]. In addition, the dye effluents cause damage to the water bodies and cause many waterborne diseases [9]. Therefore, the removal of these pollutants from drinking water is very important and several methods are utilized for the same.

The methods such as reduction, ion exchange, reverse osmosis, evaporation, and chemical precipitation are available for treatment for anions, heavy metals, organics, and dyes in drinking water sources. Many reports are available employing these techniques for reducing the amount of toxic substances in wastewater. However, most of these methods suffer from drawbacks like high capital and operational cost. In addition, there are problems in disposal of the residual metal sludge [10] which again degrade the environmental safety.

The use of activated carbons to remove organic and inorganic pollutants from water is widely extended, because of their high surface area, microporous character, and the chemical nature of their surface [11]. Commercially available activated carbons from coconut shell, lignite, peat etc. are effective for the removal of various pollutants. However, they are expensive and their regeneration cost is also high. So, there is a need for low-cost and readily available materials, such as lignocellulosic materials, for the removal of toxic pollutants from water.

Lignocellulosic materials are very porous and have a very high free surface volume that allows accessibility of aqueous solutions to the cell wall components. One cubic inch of a lignocellulosic material, for example, with a specific gravity of 0.4, has a surface area of 15 square feet. Even when the lignocellulosic material is ground, the adsorptive surface increases only slightly. Thus, the sorption of heavy metal ions by lignocellulosic materials does not depend on particle size. Lignocellulosics are hygroscopic and have an affinity for water [12–15]. Water is able to permeate the non-crystalline portion of cellulose and all of the hemicellulose and lignin. Thus, through absorption and adsorption, aqueous solution comes into contact with a very large surface area of different cell wall components.

The use of low cost and readily available agricultural wastes has to be encouraged and an attempt to use two such materials is reported here. The used materials are date palm fiber and coir pith, which are waste materials and readily processable. Coir pith is generated in the separation process of the fiber from

coconut husk. Coir pith, light to dark brown in color, consists primarily of particles in the size range 0.2–4 mm. It contains a high amount of lignin of 36%. Because of its high lignin content and amorphous, powdery nature, coir pith is one of the toughest biological materials, highly resistant to biological degradation. Utilization of coir pith for the treatment of wastewaters would be helpful not only to economy of treatments, but also for solving the solid waste disposal problems of the coir fiber industries.

Another material of importance especially for Saudi Arabia is date palm which is one of the most cultivated palms around the world. It is commonly found in the Afro-Asiatic dry-band, which stretches from North Africa to the Middle East and it has a good tolerance to cold and dry-hot climates. In the Maghreb countries, particularly in Tunisia, date palm trees cover almost 40,000 ha and represent an original form of human development in very harsh climatic conditions. Date palms have a fibrous structure, with four types of fibers: leaf fibers in the peduncle, bast fibers in the stem, wood fibers in the trunk, and surface fibers around the trunk.

Various research groups have reported the use of agro-based waste materials as adsorbents for heavy metal removal from aqueous solutions [16–18]. Ahmad et al. recently reviewed the potential of various waste products obtained from date palm tree as adsorbents for wastewater treatment [19].

Batch adsorption studies of Pb(II) on to date palm fibers were conducted by Al-Haidary et al. [20]. Riahi et al. investigated the efficacy of a column filtration system for the treatment of secondary domestic wastewater from an activated sludge treatment process, where they reported a significant reduction in turbidity, COD, phosphorous and helminth eggs in the output [21].

Coir pith and its modified forms were used for the removal of lead from aqueous solution in batch adsorption studies by various research groups [22–24]. Continuous column adsorption studies are reported to be more advantageous over batch studies in the adsorption of heavy metals from aqueous solutions using agricultural waste-based biosorbents. This is attributed to the concentration difference that exists in the column, which acts as the driving force for adsorption of heavy metals onto the surface of adsorbents [25].

This paper reports the use of agricultural waste materials, coir pith, and date palm fiber, as adsorbent for lead ions from aqueous solutions and their application in purifying the wastewater.

## 2. Materials and methods

### 2.1. Materials

#### 2.1.1. Date palm fiber

The date palm fibers were collected from the Royal commission palm tree garden. Date palm fiber was prepared in the laboratory for this investigation. The fibers were cleaned thoroughly to remove sand and dust and washed using distilled water for 20–30 times. After washing, the fibers were dried for 10 h at 80°C in a hot air oven.

The diameters of dried fibers were measured using Vernier calipers. The measured fibers were cut into different sizes ranging from 0.2 to 0.8 cm in length. The representative picture of the date palm fiber is given in Fig. 1. The different characteristics of the date palm fibers are given in Table 1.

#### 2.1.2. Coir pith

Coir pith was obtained from Devi Plantations, Kerala, India. As-received coir pith was cleaned using potable water. In order to remove the soluble particles from the coir pith, washing with distilled water was carried out. The washed coir pith was dried in air oven at 80°C for a minimum of 10 h. The characteristics of coconut coir pith are summarized in Table 2. The coconut coir pith reveals low specific surface area. In addition, the data also show that coir pith surface contains predominantly carbon and oxygen.

### 2.2. Development of the filtration column

A pilot-scale unit was set up at laboratory as shown in Fig. 2. The tank is connected by tube to the column of 100 cm long, with an inner diameter of 6 cm. At the bottom of the column, a valve with sieve

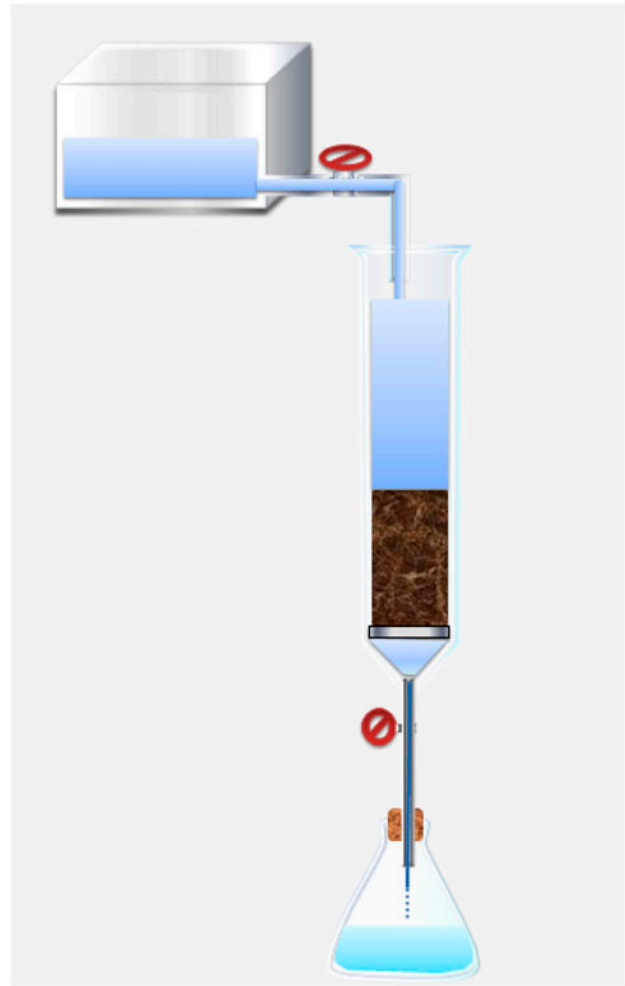


Fig. 2. Treatment system.

is fixed. The operational factors (bed material, material weight, and flow rate) employed in the present investigation are presented in Table 3.



Fig. 1. Date palm fiber after drying and cutting.

Table 1  
Characteristics of date palm fiber

Content/Property	Amount
Carbon	75.86 (wt %)
Oxygen	20.45 (wt %)
Hydrogen	2.20 (wt %)
Cobalt	0.62 (wt %)
Tensile strength	~72 MPa
Elongation	~8%
Tensile modulus	~3 (GPa)

Table 2  
Characteristics of coir pith

Parameters	Value
pH	5.58
$P_{zpc}$	7.53
Specific surface area (m <sup>2</sup> /g)	0.4290
Total pore volume (cm <sup>3</sup> /g)	0.03281
Average pore diameter (Å)	3,000.059
Element	% SEM/EDX
C	52.09
O	46.20
Cl	0.89
K	0.82

Table 3  
Design and operational conditions of adsorption materials

Bed material	Weight (g)	Flow rate mL/min
Coir pith	10	10
		50
		10
Date palm fiber	10	10
		50
		10
	20	50

### 2.2.1. Experimental procedure

Stock solution of Pb(II) was prepared in distilled water by dissolving 15.98 g of Pb<sup>2+</sup> in 10 L of water to give 500 ppm lead concentration. Adsorbent materials required for process operation were weighed and filled in the column as compact as possible. The water was allowed to flow through the column according to the flow rates. The water from the outlet was collected in every 1 min for the first 5 min and thereafter at 10, 15, 20, 40, and 60 min. The procedure was repeated for different flow rates and material weights. The bed height was calculated for each weight and it was equal to 10, 15, and 20 cm, respectively. The amount

of Pb(II) present in the sample was determined using atomic absorption spectrophotometer (AAS) (Shimadzu AA-6200) before and after treatment. Coconut coir pith and date palm fiber were analyzed by FTIR (Fourier transform infrared spectrophotometer) (4500A, Agilent) before and after treatment.

### 2.3. Mathematical modeling of breakthrough curves

Various mathematical models can be used to describe fixed-bed adsorption. Among these, the Thomas model is simple to use in the design of a fixed-bed adsorption column and the Thomas solution is one of the most general and widely used methods in column performance theory [26]. Therefore, the breakthrough data obtained from the column studies were examined using Thomas model. Successful design of a column adsorption process requires prediction of the concentration–time profile or breakthrough curve for the effluent. The maximum adsorption capacity of an adsorbent is also needed in the design. Traditionally, the Thomas model is used to fulfill the purpose. The reaction model is derived from the adsorption rate driving force which obeys second-order reversible reaction kinetics. Thomas' solution also assumes a constant separation factor, but it is applicable to either favorable or unfavorable isotherms. The primary weakness of the Thomas solution is that its derivation is based on second-order reaction kinetics. Adsorption is usually not limited by chemical reaction kinetics, but is also often controlled by inter-phase mass transfer. This discrepancy can lead to some error when this method is used to model adsorption. The expression of the Thomas model for an adsorption column is as follows:

$$\frac{C_t}{C_0} = \frac{1}{1 + \exp((k_{TH}/Q)(q_0X - C_0V_{eff}))} \quad (1)$$

where  $k_{TH}$  is the Thomas rate constant (m/min/mg),  $q_0$  the maximum solid-phase concentration of the solute (mg/g),  $V_{eff}$  the effluent volume (ml),  $X$  the mass of adsorbent (g), and  $Q$  the flow rate (mL/min).

The liberalized form of the Thomas model is as follows:

$$\ln\left(\frac{C_0}{C_t} - 1\right) = \frac{k_{TH}q_0X}{Q} - \frac{kC_0V_{eff}}{Q} \quad (2)$$

The kinetic coefficient  $k_{TH}$  and the adsorption capacity of the bed  $q_0$  can be determined from a plot of  $\ln[(C_0/C_t) - 1]$  against  $t$  at given conditions. The

breakthrough curves show the superposition of experimental results (points) and the theoretically calculated points (lines). Linear regression coefficients  $R^2$  show the fit between experimental data and liberalized forms of Thomas equation while the average percentage errors ( $\epsilon$  %) calculated according to Eq. (3) indicate the fit between the experimental and predicted values of  $C_t/C_0$  used for plotting breakthrough curves.

$$\epsilon = \frac{\sum_{i=1}^N [((C_t/C_0)_{\text{exp}} - (C_t/C_0)_{\text{theo}})/(C_t/C_0)_{\text{exp}}]}{N} \times 100 \quad (3)$$

where  $N$  is the number of measurements [27]. The application of Thomas model is described in various fixed-bed systems of adsorption [28,29].

### 3. Results and discussion

#### 3.1. Fourier transform infrared spectroscopy (FTIR)

The FTIR spectra before and after adsorption on coir pith are shown in Fig. 3 and those for date palm fiber are shown in Fig. 4. The functional groups before and after adsorption on coir pith and date palm fiber and the corresponding infrared absorption frequencies are shown in Tables 4 and 5, respectively.

As shown in Fig. 3 and Table 4, the spectra display a number of absorption peaks, indicating the complex nature of coir pith. The FTIR spectroscopic analysis indicated broadbands at  $3,340 \text{ cm}^{-1}$ , representing bonded  $-\text{OH}$  groups. The bands observed at about  $2,916 \text{ cm}^{-1}$  could be assigned to the aliphatic  $\text{C}-\text{H}$

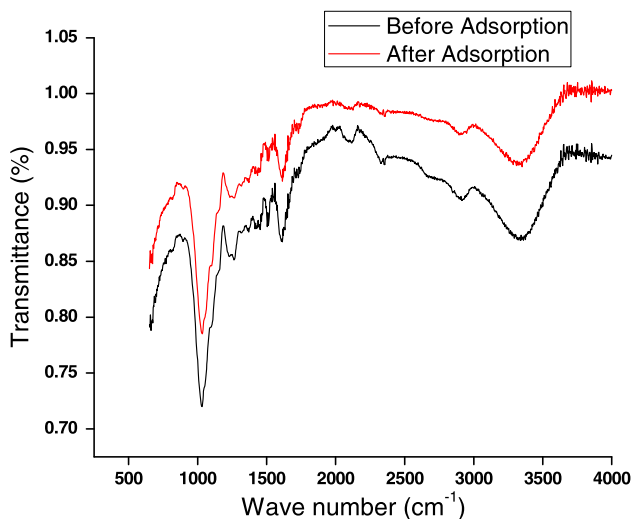


Fig. 3. FTIR spectra for coir pith before and after adsorption.

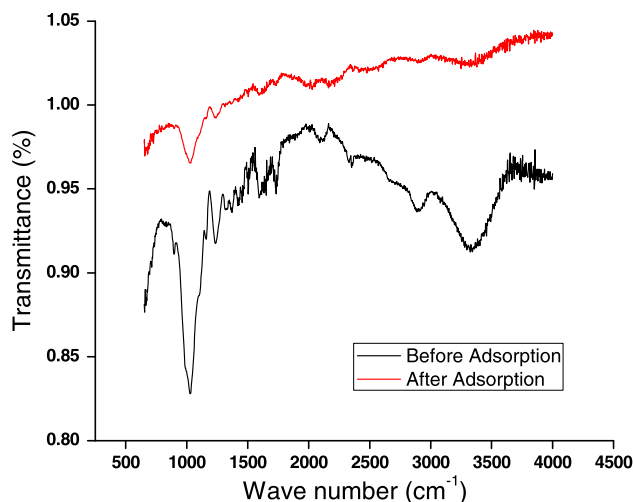


Fig. 4. FTIR spectra for date palm fiber before and after adsorption.

group. The peak around  $1,730 \text{ cm}^{-1}$  corresponds to the  $\text{C}=\text{O}$  stretch. The peaks observed at  $1,232$ ,  $1,141$ , and  $1,030$  and  $614 \text{ cm}^{-1}$  could be assigned to  $-\text{SO}_3$  stretching,  $\text{C}-\text{O}$  stretching of ether groups,  $-\text{C}-\text{C}$  group, and  $-\text{CN}$  stretching, respectively. As seen in Table 4, the spectral analysis before and after metal adsorption indicated that most of the peaks remain the same and hence the adsorption of lead onto coir pith is mostly by physisorption rather than chemisorption.

The FTIR spectra before and after adsorption of lead onto date palm fibers are shown in Fig. 4. The functional groups before and after adsorption studies and the corresponding infrared absorption bands are shown in Table 5. The spectra display a number of absorption peaks, indicating the complex nature of date palm fibers. The band shifts corresponding to  $-\text{OH}$  groups,  $\text{C}-\text{H}$  groups, and  $\text{C}-\text{O}$  groups indicate that the adsorption of lead on date palm fibers come under the category of chemisorption, and mainly  $-\text{OH}$  groups are involved in the chemisorption process.

#### 3.2. Adsorption by date palm fibers

##### 3.2.1. Effect of flow rate

The effect of flow rate on the adsorption kinetics of  $\text{Pb}(\text{II})$  by date palm fibers was studied experimentally by keeping initial  $\text{Pb}(\text{II})$  concentration as  $155 \text{ mg/L}$  and mass of adsorbent as  $10 \text{ g}$ . The experiments were conducted at flow rates of  $10$  and  $50 \text{ mL/min}$ . The breakthrough curves are presented in Fig. 5(a). From the breakthrough curves, a rapid adsorption was observed at higher flow rate. This indicates that the occupancy of the available adsorption sites is faster at

Table 4  
FTIR spectral characteristics of coir pith before and after adsorption studies

IR peak	Frequency ( $\text{cm}^{-1}$ )			Assignment
	Before adsorption	After adsorption	Difference	
1	3,340	3,340	0	–OH
2	2,916	2,910	–6	C–H
3	1,730	1,730	0	C=O
4	1,610	1,612	+2	C=C
5	1,425–1,265	1,425–1,265	0	C–O–H
6	1,030	1,030	0	–C–C– group

Table 5  
FTIR spectral characteristics of date palm fiber before and after adsorption studies

IR peak	Frequency ( $\text{cm}^{-1}$ )			Assignment
	Before adsorption	After adsorption	Difference	
1	3,341	3,324	–17	–OH
2	2,895	2,898	+3	Aliphatic C–H groups
3	1,233	1,236	+3	C–O stretching

higher flow rates. The results presented in Fig. 5(a) show that the breakthrough curve is sharper with increase in the flow rate. At lower flow rate the

breakthrough curve is steeper. Another important observation is that the break point time decreases at higher flow rate. This indicates that equilibrium is attained rapidly and even though the contact time is low, the adsorption efficiency is very high.

The effect of flow rate was studied for the same adsorption system, but with increase in the mass of adsorbent in the column to 20 g. The results obtained are depicted in Fig. 5(b). It can be concluded from Fig. 5(b) that initially the adsorption was very rapid (within 5 min) at higher flow rate (50 mL/min). This is probably associated with the ability of the reaction sites on the surface of the date palm fibers to capture metal ions. After 5 min, the uptake of lead ions on date palm fibers becomes less effective due to the occupancy of the active sites with lead ions. As Fig. 5(b) displays, at lower flow rates (10 mL/min), the occupancy of the active sites needs longer time (20 min) to reach the break point and the breakthrough curve becomes steeper. Fig. 5(b) shows that the exhaustion time decreases with increasing the flow rate from 10 to 50 mL/min.

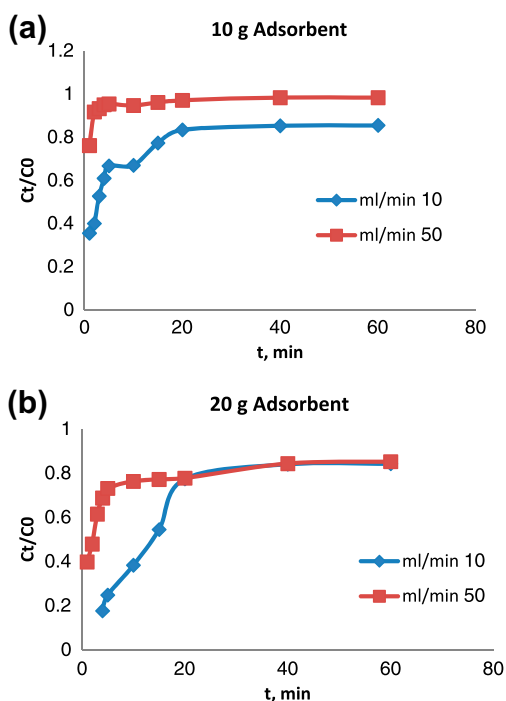


Fig. 5. Breakthrough curves for Pb(II) adsorption by date palm fibers at different flow rates (initial Pb(II) concentration = 155 mg/L), mass of adsorbent (a) 10 g, and (b) 20 g.

### 3.2.2. Mathematical modeling of breakthrough curves

The obtained experimental data shown in Fig. 5 were evaluated using Thomas model in order to understand the adsorption column parameters. The linear plot of the experimental data according to Thomas model (Eq. (3)) at flow rates of 10 and 50 mL/min is presented in Fig. 6. As Fig. 6 shows, the Thomas model

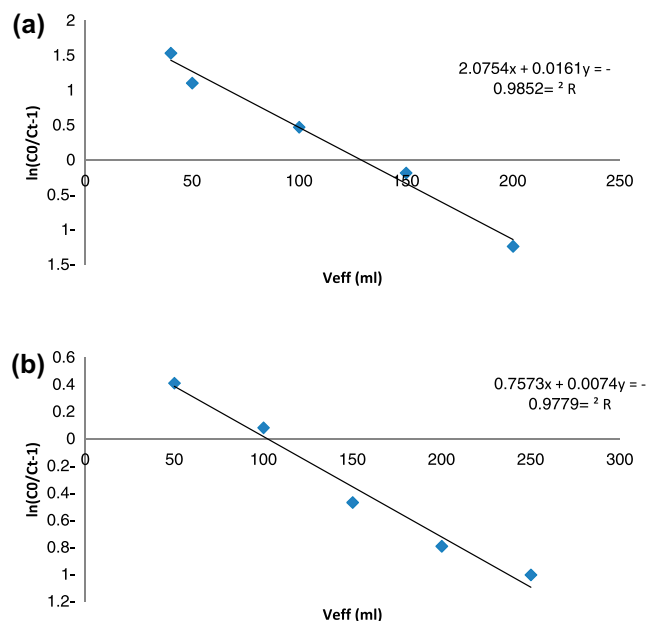


Fig. 6. The linear plot of the experimental adsorption data according to Thomas model at the flow rates (a): 10 mL/min; (b): 50 mL/min (initial Pb(II) concentration = 155 mg/L, mass of adsorbent = 20 g).

gives a good fit of the measured adsorption breakthrough curves for adsorption of Pb(II) on date palm fibers. The effect of flow rate on the column adsorption parameters such as Thomas constant ( $k_{TH}$ ) and the maximum solid phase concentration of the solute ( $q_{eq}$ ) can be determined from the slopes and intercepts of the linear plots in Fig. 7. The results are presented in Table 6.

As seen in Table 6, the total adsorbed lead quantity, maximum lead uptake, and lead removal percentage values increased with increasing flow rate.

### 3.3. Adsorption by coir pith

The dependence of flow rate on the adsorption kinetics of Pb(II) by coir pith was studied experimentally by keeping the initial Pb(II) concentration (155 mg/L) as constant and selecting two different masses of adsorbent (10 and 20 g). The experiments were conducted at flow rate values of 10 and 50 mL/min. The results are shown in Fig. 7. From the figure, it can be observed that in the case of 10 g adsorbent for both flow rates, the breakthrough point was obtained after 20 min. This can be attributed to the availability of more active sites in the first 20 min. After reaching the breakthrough point, the number of active sites decreases and the adsorption becomes

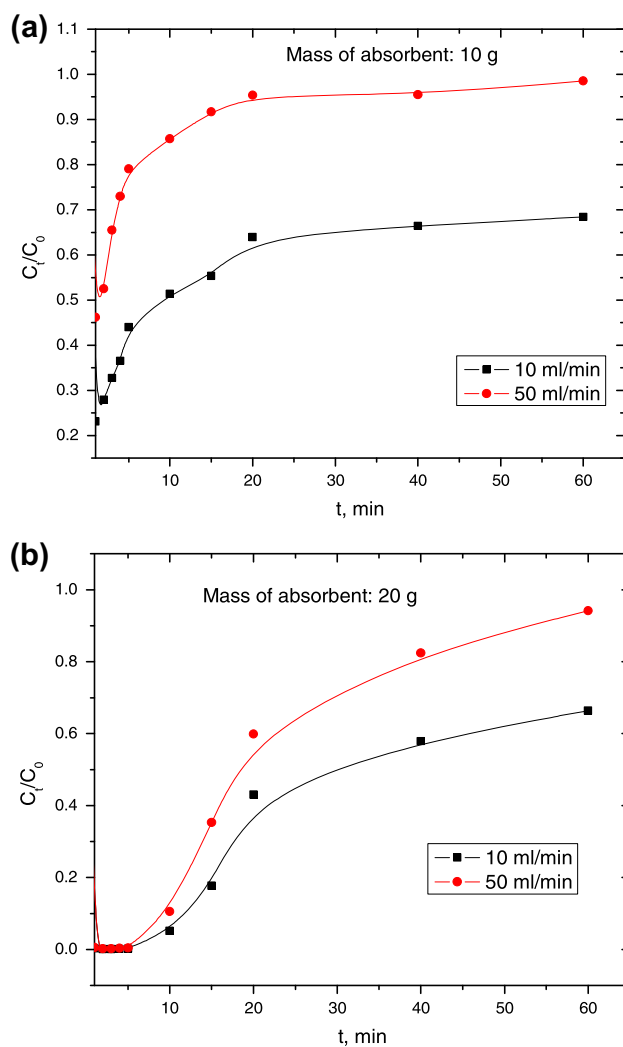


Fig. 7. Breakthrough curve for Pb(II) adsorption by coir pith (initial Pb(II) concentration = 135 mg/L), mass of adsorbent (a) 10 g and (b) 20 g.

constant. However, when the mass of the adsorbent is increased to 20 g, the breakthrough point is 40 min, which shows that more active sites are available up to that time.

Fig. 8 shows the linear plot of the experimental adsorption data according to Thomas model (Eq. (3)) at flow rates of 10 and 50 mL/min. As Fig. 8 shows, Thomas model gives good fit for the measured adsorption breakthrough curves for adsorption of Pb(II) on coir pith.

### 3.4. Comparison of coir pith with date palm fibers

A plot of the breakthrough curves for the adsorption of Pb(II) ions by coir pith and date palm fibers

Table 6

The effect of flow rate on the total absorbed quantity of Pb(II), equilibrium uptake, and total removal percentage by date palm fibers (initial Pb(II) concentration = 155 mg/L, mass of adsorbent = 20 g)

Flow rate (mL/min)	$k_{TH}$ (mL/min mg)	$q_{eq}$ (mg/g)	$q_{total}$ (mg)	Total metal removal (%)	Correlation coefficient
10	10.32258	0.100508	2.010152	2.161	0.985
50	2.258065	2.297326	45.94652	9.881	0.977

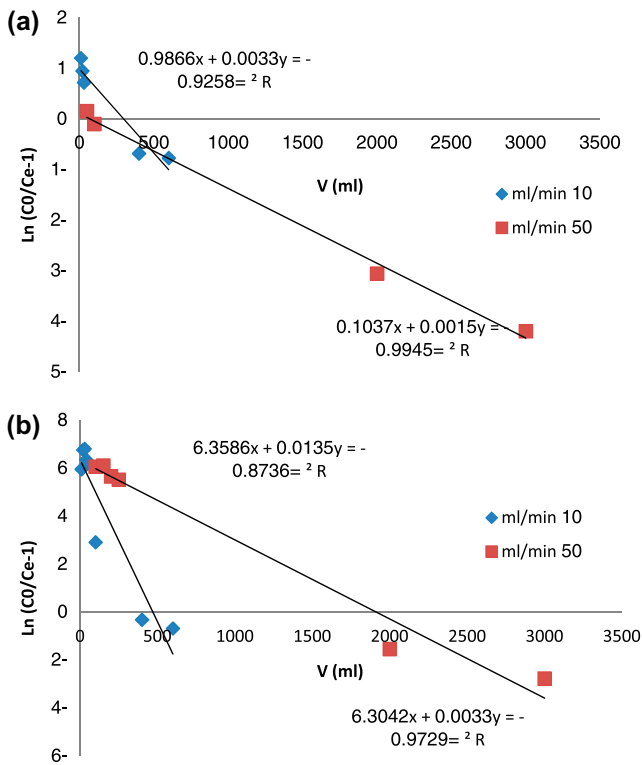


Fig. 8. The linear plot of the experimental adsorption data according to Thomas model (initial Pb concentration = 135 mg/L), mass of adsorbent (a) 10 g and (b) 20 g.

under identical conditions is presented in Fig. 9. It is clear from the figure that in the case of date palm fibers, the breakthrough point was 3 min, which is much less than the breakthrough point of coir pith (20 min). This gives clear evidence that the occupancy rate of date palm fibers with Pb(II) ions is faster than that of coir pith. Therefore, further studies were conducted with date palm fibers.

### 3.4.1. Effect of flow rate

The effect of different flow rates was studied by keeping the other parameters constant such as the column height to 10 cm, mass of the adsorbent to 26 g, and the initial concentration of 135 mg/L of Pb(II) ion

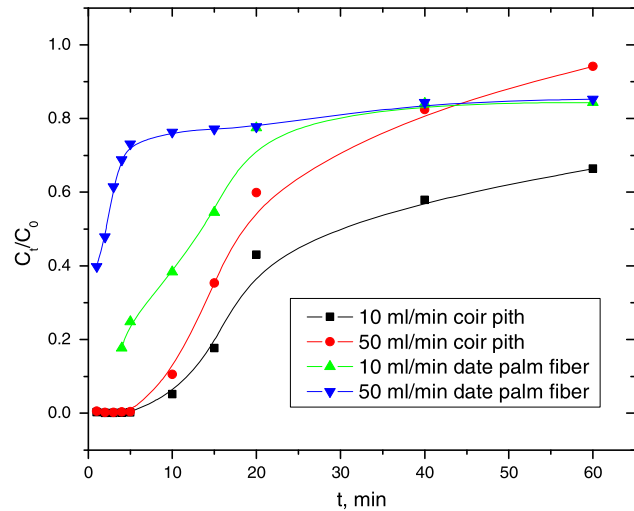


Fig. 9. Breakthrough curve for Pb(II) adsorption onto coir pith and date palm fibers (initial Pb(II) concentration = 135–155 mg/L, mass of adsorbent = 20 g).

solution. Three different flow rates of 3, 10, and 20 mL/min were used. The corresponding breakthrough curves and the Thomas model curves are given in Fig. 10. The breakthrough curves show that the optimum flow rate is close to 10 mL/min as there is no major difference in trend between 10 and 20 mL/min. However, there is sharp difference between the curves for 3 and 10 mL/min. This difference is also reflected in the Thomas model curves and parameters. The nature of the curves for 10 and 20 are similar and is quite different for 3 mL/min. Moreover, the different parameters for Thomas model have been calculated and it helps to have good understanding about the effect of flow rate on the adsorption behavior. The corresponding values for  $k_{TH}$  for 3, 10, and 20 mL/min are 0.03, 0.04, and 0.08, respectively, which shows sharp difference for the latter flow rates. Other two parameters,  $q_0$  and  $R^2$  for the flow rates being investigated are 21, 52, 52, and 0.964, 0.962, 0.994, respectively. In short, it can be concluded that the date palm fiber gives optimum adsorption properties around 10 mL/min for this kind of setup.

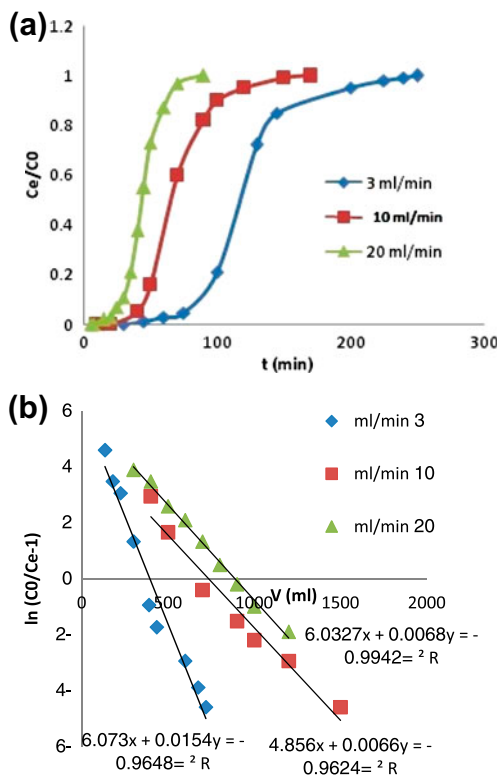


Fig. 10. (a) The breakthrough curves showing the effect of flow rate and (b) The linear plot of the experimental adsorption data according to Thomas model (flow rate 3, 10, 20 mL/min) for date palm fiber.

### 3.4.2. Effect of initial concentration

The effect of change in initial concentration was studied by keeping the other parameters constant such as the column height to 10 cm, mass of the adsorbent to 26 g, and the flow rate to 10 mL/min. Three different initial concentrations of 80, 135, and 200 mg/L were used to analyze the behavior. The breakthrough curves and the Thomas model curves are given in Fig. 11. The breakthrough curves show that according to the initial concentration, the nature of the curve changes. For 80 mg/L, the curve shows an initial residence time and thereafter the curve becomes steeper. This initial residence behavior is reduced in the case of 135 mg/L and it is not observed in 200 mg/L. Therefore, the optimum initial concentration falls in the range of 135 mg/L. This difference is also reflected in the Thomas model curves and parameters. The nature of the curves is similar for all the three initial concentrations. Moreover, the different parameters for Thomas model have been calculated, and it gives good idea about the effect of initial concentration on the adsorption behavior. The corresponding values for  $k_{TH}$  for 80, 135, and 200 mg/L are 0.075, 0.0444, and 0.035,

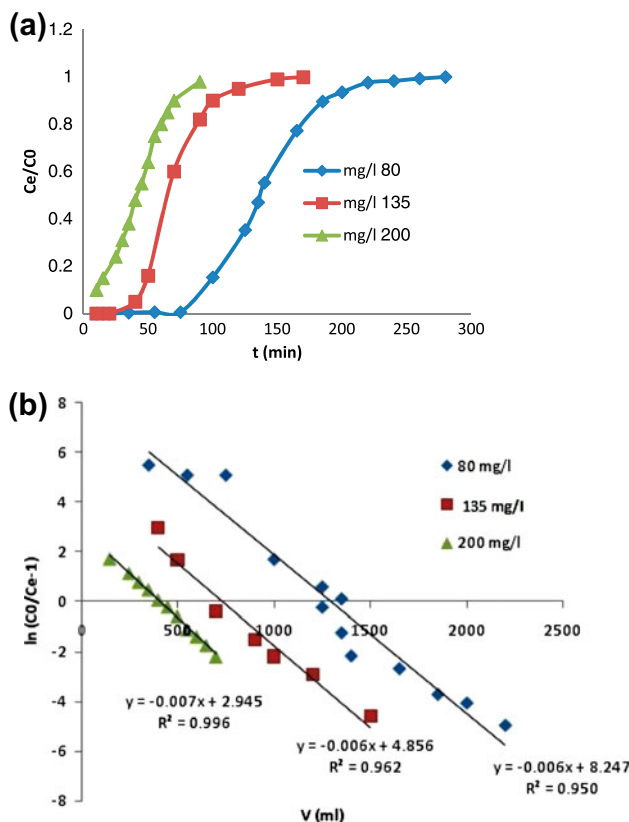


Fig. 11. (a) The breakthrough curves showing the effect of initial concentration and (b) The linear plot of the experimental adsorption data according to Thomas model (initial concentration of 80, 135, 200 mg/min) for date palm fiber.

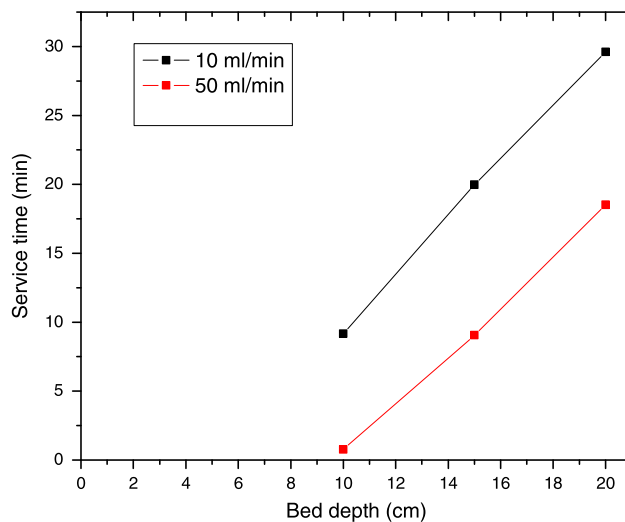


Fig. 12. BDST plot for coir pith at two different flow rates of 50% breakthrough (concentration of metal ion: 135 mg/L).

Table 7  
Parameters from BDST plots.

Material	Volume flow rate (mL/min)	Slope $m$ (min/cm)	Y-intercept $b$ (min)	X-intercept $Z_0$ (cm)	Correlation coefficient ( $r^2$ )
Coir pith	10	2.04	11.09	5.2	0.9994
	50	1.77	17.18	9.5	0.9996
Date palm fiber	10	0.5	2.23	4.5	0.9999
	50	0.22	2.35	10.9	0.9999

respectively, which shows sharp difference for the latter values compared to the first one. Other two parameters deduced from Thomas model,  $q_0$  and  $R^2$ , are 42.292, 51.568, 61.2 and 0.95, 0.962, 0.996, respectively. It can be concluded that the date palm fiber gives optimum adsorption properties for the initial concentration of 135 mg/L.

### 3.4.3. Critical bed depth

Critical bed depth is defined as the minimum depth for obtaining satisfactory effluent at time zero under the test operating conditions [30]. In order to find out the critical bed depth, bed depth service time (BDST) curves were plotted for both date palm fiber and coir pith as adsorbents. Fig. 12 shows the BDST curve for coir pith in three different bed heights at two different flow rates (10 and 50 mL/min) and a breakthrough of 50%. The variations of the curves and the constants demonstrate that the two materials have different sorption capacities. The slopes and intercepts for the BDST plots for different process variables are shown in Table 7.

The service time,  $t$ , and the bed depth,  $Z$ , can be correlated with the process parameters such as initial solute concentration, the solution flow rate, the adsorption capacity, and the adsorption rate constant. Hutchins suggested an equation to find out BDST in the form of a straight line ( $y = mx + c$ ) [31]. Thus, the slope of the BDST plot is the time required to exhaust a unit length of the sorbent in the column under the test condition. The intercept on the ordinate,  $b$ , is the time required for the adsorption wave front to pass through the critical bed depth. From Table 7, it can be concluded that the slope for both materials decreases with respect to increase in flow rate. Similar reports were reported by Walker and Weatherley for adsorption of acid dyes on activated carbon [32].

The  $y$ -intercept  $b$  shows an increase with respect to flow rate which is expected as the time to adsorb the metal becomes low. The critical bed depth  $Z_0$ , showed an increase with increase in flow rate, with the minimum bed depth required for adequate Pb(II) adsorption

increasing by approximately 50% for the materials with a fivefold increase in flow rate. These results correlate well with the observed performance in the breakthrough curves. The correlation coefficient  $r^2$ , values calculated for the linearization of the experimental data were generally quite high, with values all above 0.994. The advantage of elucidating BDST model parameters is that the data can be used as such for scaling up of the process with different flow rates without experimental trials [33].

## 4. Conclusion

A laboratory filtration setup was made using date palm fiber and coir pith as adsorbents. Adsorption of Pb(II) onto these adsorbents was monitored continuously. The operating parameters employed were flow rate and weight of the adsorbent. AAS was used to measure the Pb(II) concentration in the water before and after each experiment. The adsorbent materials were analyzed using FTIR spectrometer before and after the studies. Thomas model, which is the commonly used mathematical model for continuous column filtration studies, was applied to study the efficiency of the adsorbent materials. It was observed that for date palm fibers, the breakthrough point was 3 min which is much less than the breakthrough point in the case of coir pith (20 min). This gives clear evidence that the occupancy rate of date palm fibers with Pb(II) ions is faster than that of coir pith. The adsorption data revealed that the adsorption capacity of date palm fibers is higher than that of coir pith at all flow rates. The FTIR studies showed that the adsorption of Pb(II) on date palm fibers comes under the category of chemisorption and mainly –OH groups are involved in the process. However, the adsorption process with respect to coir pith is believed to be due to physisorption. The effect of flow rate and initial concentration on the adsorption process was studied with date palm fibers and a flow rate of 10 mL/min and an initial concentration of 135 mg/L were found as optimum values. The use of agricultural waste materials as heavy metal adsorbent, as evidenced from

the results of the present study, could be thought of as a viable alternative to make sustainable and economic wastewater treatment systems.

## References

- [1] N.F. Gray, *Drinking Water Quality*, second ed., Cambridge University Press, New York, NY, 2008.
- [2] D. Mara, *Domestic Wastewater Treatment in Developing Countries*, Earthscan Publishers, Sterling, 2004.
- [3] V. Mavrov, A. Fähnrich, H. Chmiel, Treatment of low-contaminated waste water from the food industry to produce water of drinking quality for reuse, *Desalination* 113 (1997) 197–203.
- [4] IS 10500. Quality criteria for drinking water, Bureau of Indian Standards, New Delhi, 1989.
- [5] US EPA. National Primary Drinking Water Regulations, EPA, Washington, DC, 1996.
- [6] A. Kabata-Pendias, H. Pendias, *Biochemistry of Trace Elements*, PWN, Warsaw, 1993.
- [7] R. Hartung, Cyanides and nitriles, in: G.D. Clayton, E. Clayton (Eds.), *Patty's Industrial Hygiene and Toxicology*, vol. 2C, John Wiley & Sons, New York, NY, 1982, pp. 4845–4900.
- [8] A.L. Buikema, M.J. McGinniss, J. Cairns, Phenolics in aquatic ecosystems: A selected review of recent literature, *Mar. Environ. Res.* 2 (1979) 87–181.
- [9] R.J. Maguire, Occurrence and persistence of dyes in a Canadian river, *Water Sci. Technol.* 25 (1995) 265–270.
- [10] D.C. Sharma, C.F. Forster, A preliminary examination into the adsorption of hexavalent chromium using low-cost adsorbents, *Bioresour. Technol.* 47 (1994) 257–264.
- [11] I. Bautista-Toledo, J. Rivera-Utrilla, M.A. Ferro-García, C. Moreno-Castilla, Influence of the oxygen surface complexes of activated carbons on the adsorption of chromium ions from aqueous solutions: Effect of sodium chloride and humic acid, *Carbon* 32 (1994) 93–100.
- [12] P.A. Sreekumar, S.P. Thomas, J. Marc Saiter, K. Joseph, G. Unnikrishnan, S. Thomas, Effect of fiber surface modification on the mechanical and water absorption characteristics of sisal/polyester composites fabricated by resin transfer molding, *Composites Part A: Appl. Sci. Manuf.* 40 (2009) 1777–1784.
- [13] H.N. Dhakal, Z.Y. Zhang, M.O.W. Richardson, Effect of water absorption on the mechanical properties of hemp fibre reinforced unsaturated polyester composites, *Compos. Sci. Technol.* 67 (2007) 1674–1683.
- [14] A. Espert, F. Vilaplana, S. Karlsson, Comparison of water absorption in natural cellulosic fibres from wood and one-year crops in polypropylene composites and its influence on their mechanical properties, *Composites Part A: Appl. Sci. Manuf.* 35 (2004) 1267–1276.
- [15] D.N. Saheb, J.P. Jog, Natural fiber polymer composites: A review, *Adv. Polym. Technol.* 18 (1999) 351–363.
- [16] A. Demirbas, Heavy metal adsorption onto agro-based waste materials: A review, *J. Hazard. Mater.* 157 (2008) 220–229.
- [17] D. Sud, G. Mahajan, M.P. Kaur, Agricultural waste material as potential adsorbent for sequestering heavy metal ions from aqueous solutions—A review, *Bioresour. Technol.* 99 (2008) 6017–6027.
- [18] S. Babel, T.A. Kurniawan, Low-cost adsorbents for heavy metals uptake from contaminated water: A review, *J. Hazard. Mater.* 97 (2003) 219–243.
- [19] T. Ahmad, M. Danish, M. Rafatullah, A. Ghazali, O. Sulaiman, R. Hashim, M.N.M. Ibrahim, The use of date palm as a potential adsorbent for wastewater treatment: A review, *Environ. Sci. Pollut. Res.* 19 (2012) 1464–1484.
- [20] A.M.A. Al-Haidary, F.H. Zanganah, S.R. Al-Azawi, F.I. Khalili, A.H. Al-Dujaili, A study on using date palm fibers and leaf base of palm as adsorbents for Pb (II) ions from its aqueous solution, *Water Air Soil Pollut.* 214 (2011) 73–82.
- [21] K. Riahi, A.B. Mammou, B.B. Thayer, Date-palm fibers media filters as a potential technology for tertiary domestic wastewater treatment, *J. Hazard. Mater.* 161 (2009) 608–613.
- [22] P. Kumar, R. Rao, S. Chand, S. Kumar, K.L. Wasewar, C.K. Yoo, Adsorption of lead from aqueous solution onto coir-pith activated carbon, *Desalin. Water Treat.* 51 (2013) 2529–2535.
- [23] K. Wantala, N. Pojananukij, P. Sriprom, T. Kumsaen, A. Neramittagapong, S. Neramittagapong, Metal adsorbent prepared from coir pith as agricultural waste: Adsorption of Zn(II) and Pb(II) from aqueous solution, *Key Eng. Mater.* 545 (2013) 101–108.
- [24] C. Namasivayam, D. Sangeetha, Recycling of agricultural solid waste, coir pith: Removal of anions, heavy metals, organics and dyes from water by adsorption onto ZnCl<sub>2</sub> activated coir pith carbon, *J. Hazard. Mater.* 135 (2006) 449–452.
- [25] K.H. Chu, Improved fixed bed models for metal biosorption, *Chem. Eng. J.* 97 (2004) 233–239.
- [26] P. Persoff, J.F. Thomas, Estimating Michaelis-Menten or Langmuir isotherm constants by weighted nonlinear least squares, *Soil Sci. Soc. Am. J.* 52 (1988) 886–889.
- [27] A.P. Henderson, L.N. Seetohul, A.K. Dean, P. Russell, S. Pruneanu, Z. Ali, A novel isotherm, modelling self-assembled monolayer adsorption and structural changes, *Langmuir* 25 (2009) 931–938.
- [28] R.P. Han, Y. Wang, W.H. Zou, Y.F. Wang, J. Shi, Comparison of linear and nonlinear analysis in estimating the Thomas model parameters for methylene blue adsorption onto natural zeolite in fixed-bed column, *J. Hazard. Mater.* 145 (2007) 331–335.
- [29] Z. Xu, J. Cai, B. Pan, Mathematically modeling fixed-bed adsorption in aqueous systems, *J. Zhejiang Univ. Sci. A (Appl. Phys. Eng.)*, 14 (2013) 155–176.
- [30] S. Ghorai, K.K. Pant, Equilibrium, kinetics and breakthrough studies for adsorption of fluoride on activated alumina, *Sep. Purif. Technol.* 42 (2005) 265–271.
- [31] R.A. Hutchins, New method simplifies design of activated carbon systems, *Chem. Eng.* 80 (1973) 133–138.
- [32] G.M. Walker, L.R. Weatherley, Adsorption of acid dyes on to granular activated carbon in fixed beds, *Water Res.* 31 (1997) 2093–2101.
- [33] B. Sivaprakash, N. Rajamohan, A.M. Sathik, Batch and column sorption of heavy metal from aqueous solution using a marine alga *Sargassum tenerimum*, *Int. J. ChemTech Res.* 2 (2010) 155–162.